Research Article

# In-Silico Molecular Docking and Pharmaco-Kinetic Activity Analysis of Potential Inhibitors against SARS-CoV-2 Spike Glycoproteins

**Mita Shikder[1], Kazi Ahsan Ahmed[1*] iD, Tasnin Al Hasib[1], Pranta Ray[2], Abul Bashar Ripon Khalipha[2], Md. Lutful Kabir[1]**

[1]Department of Biochemistry and Molecular Biology, Life Science Faculty, Bangabandhu Sheikh Mujibur Rahman Science and Technology University, Gopalganj, Bangladesh
[2]Department of Pharmacy, Life Science Faculty, Bangabandhu Sheikh Mujibur Rahman Science and Technology University, Gopalganj, Bangladesh
 E-mail: kaziahsanahmed.bmb@gmail.com

**Abstract:** Severe Acute Respiratory Syndrome Coronavirus 2 (SARS-COV-2) is a causative agent of the potentially fatal coronavirus disease (COVID-19). Coronavirus targets the human respiratory system primarily. It can also infect the gastrointestinal, hepatic, and central nervous systems of humans, avians, bats, livestock, mice, and many other wild animals, as these are primary targets of the pathogen. This study aims to screen out the most potent inhibitor for SARS-CoV-2 (COVID-19) spike glycoproteins among the selected drugs, and computational tools have been utilized for this purpose. The selected drugs have been designed to explore their structural properties in this study by molecular orbital calculation. To inhibit the spike glycoproteins, the performance of these drugs was also examined by molecular docking calculation. In improving the performance of drugs, non-bond interactions play a significant role. To determine the chemical reactivity of all the medicines, HOMO and LUMO energy values were also calculated. The combined calculations exhibited that Ledipasvir among the selected drugs can be the most potent drug to treat SARS-CoV-2 compared to other medications.

*Keywords*: severe acute respiratory syndrome coronavirus 2 (SARS-CoV-2), COVID-19, Ledipasvir, molecular docking, molecular orbital calculation

## 1. Introduction

The rapid outbreak of coronavirus disease (COVID-19) was first identified in December 2019 where the ongoing pandemic had started [1]. It is caused by a newly emerged virus, severe acute respiratory syndrome coronavirus 2 (SARS-CoV-2) [2]. More than 11 million cases of COVID-19 disease have been reported in more than 188 countries, resulting in more than half a million deaths reported by 6 July, 2020 [3]. Unfortunately, there is no specific and effective medicine or treatment for this pandemic disease [4]. Drug discovery, drug development, and therapeutic measures are needed immediately to control the SARS-CoV-2 outbreak.

The COVID-19 virus is a single-stranded, positive-sense RNA virus related to SARS and MERS coronavirus [5]. The genome of the SARS-CoV virus family encodes four structural proteins such as spike glycoproteins, envelope

protein, membrane protein and nucleocapsid protein [6]. Among them, spike glycoproteins allow interaction between virus and cell receptors during viral entry into the host cell [7]. The main target of spike glycoproteins is to neutralize antibodies by binding with their receptors [8]. Thus, the spike glycoprotein plays a significant role in viral entry into the host cell.

This study deals with the identification of potential inhibitors against spike glycoprotein of SARS-CoV-2 using the computational method of drug design. In structural molecular biology and Computer-Aided Drug Designing (CADD), Molecular Docking is used for protein docking to predict the binding mode(s) of a ligand with a protein [9]. Molecular docking is a computational procedure that helps to forecast the binding of the macromolecule (receptor) and a small molecule (ligand) very effectively [10]. The information obtained from the docking technique can be used to point out the binding energy, free energy, and stability of complexes, and hence this technique has given the advantages to predict the probable binding parameters of the receptor complex [11]. The small molecules denoted as the ligand and their binding affinity with the receptor are very important because they are used to screen virtual libraries of drug-like molecules to predict the best candidate with the aim of drug development [12]. A molecular receptor's binding capability with a ligand depends on a few parameters as molecular recognition, known as non-bond interaction. These are useful parameters for structure-based drug design in structural biology and pharmaceutical chemistry [13, 14].

Properties of some potential drugs have been scrutinized in this study against SARS-CoV-2 spike glycoprotein [PDB IDs: 6LZG (Chain B), 6VXX (Chain A), 6X29 (Chain A), 6YM0 (Chain E), 6YOR (Chain E)] in order to inhibit the infection caused by severe acute respiratory syndrome coronavirus 2 [15, 16]. Most of these drugs are HIV Protease Inhibitor. The drug Hypericin is considered as antineoplastic agent, antiviral agent, enzyme inhibitor, immunosuppressive agent, radiation-sensitizing agent, anti-depressive agent. Beclabuvir is considered as an HCV Protease Inhibitor. Ledipasvir also plays a significant role as a direct-acting antiviral agent (DAA). Among these drugs, Conivaptan, Inosine. Lentinan and Nystatin are non-antiviral but highly active against SARS-CoV-2 spike glycoproteins [17].

In this study, we employ binding affinity and non-bond interaction of potential drugs against SARS-CoV-2 spike glycoprotein. Pharmaco-kinetic properties and frontier molecular orbitals of those drugs are also explored in detail. Molecular docking has predicted a better binding affinity of some drugs with the target molecules.

# 2. Materials and computational methodology

## 2.1 Collection of ligands

Two-dimensional structures of the ligands were retrieved from the PubChem project in SDF format. They are anti-viral drugs, except the four: Conivaptan, Inosine, Lentinan, and Nystatin. The brief description and the 2D structures of the drugs considered in this study were given in Table 1 below.

## 2.2 Preparation of target protein for molecular docking

The drugs were subjected to molecular docking against SARS-CoV-2 spike glycoprotein [PDB IDs: 6LZG (Chain B) [18], 6VXX (Chain A) [19], 6X29 (Chain A) [20], 6YM0 (Chain E) [21], 6YOR (Chain E) [22]]. The crystal structure of these proteins was collected from Protein Data Bank (PDB) online database. The unwanted ions, ligands, and water molecules were removed from these proteins by using PyMOL software [23]. Energy minimization of optimized proteins structure was obtained by using Swiss-PDB Viewer [24]. Finally, the minimized protein structure was saved in PDB format.

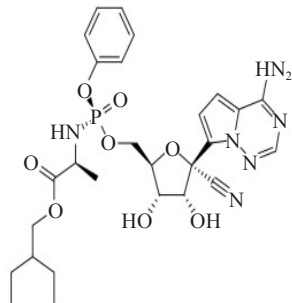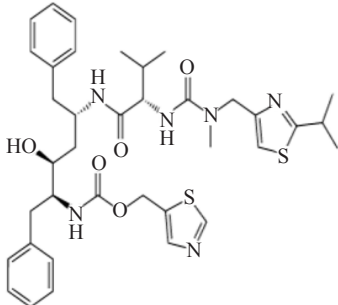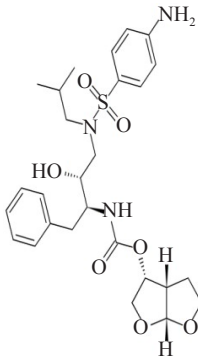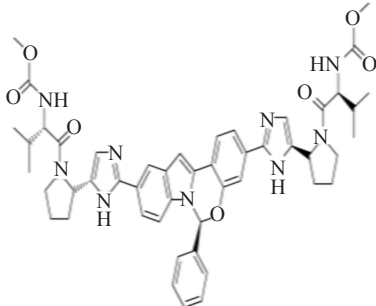## 2.3 Drug optimization using calculation of molecular orbital

The molecular orbital calculation, also known as frontier molecular orbital calculation, was done using the webMO database. HOMO and LUMO are the acronyms of the highest occupied molecular orbital and lowest unoccupied molecular orbital, respectively. The term HOMO-LUMO gap is the energy difference between HOMO and LUMO [25]. HOMO-LUMO difference <1.3 indicates the higher chemical reactivity of the molecule [26]. HOMO-LUMO is an indication of the chemical hardness and softness of the molecule. Hardness indicates the aptitude of electrostatic
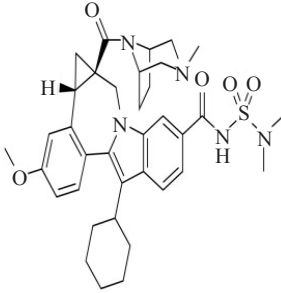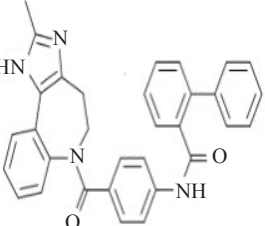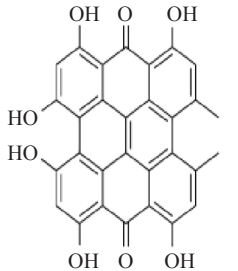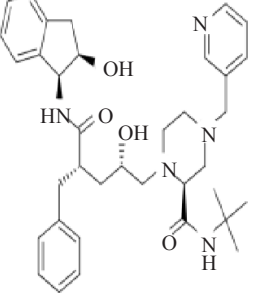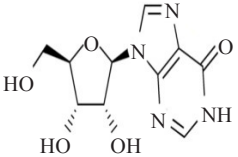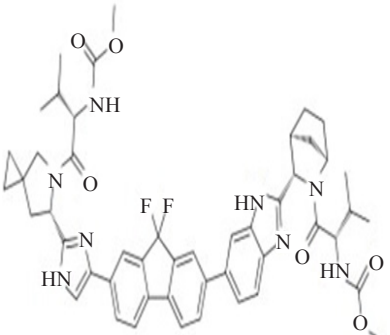
interaction, and softness indicates the reactivity by electron transfer [27]. Hardness (η) and softness (S) of the ligands were calculated by using Parr and Pearson interpretations [28].
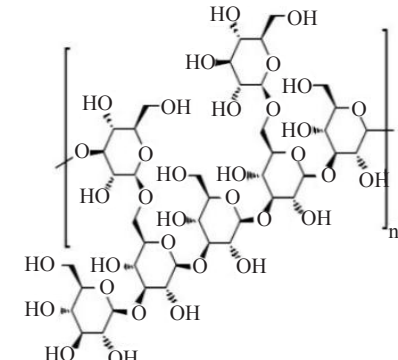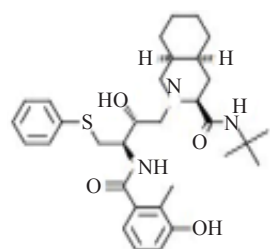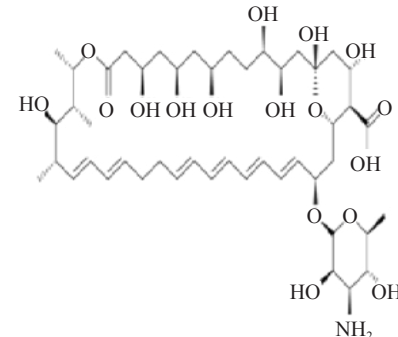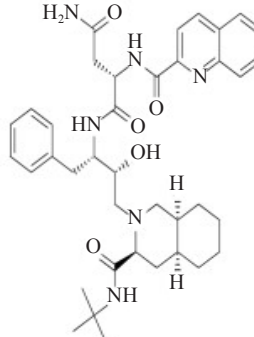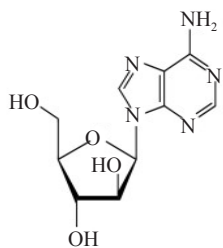
$$\eta = (\varepsilon LUMO - \varepsilon HOMO)/2 \tag{1}$$

$$S = 1/\eta \tag{2}$$

**Table 1.** The drugs that were considered in this study with a brief description

| PubChem CID | Ligands | Indication | Groups | 2D structure | Reference |
|---|---|---|---|---|---|
| 121304016 | Remdesivir | • Antimetabolites<br>• Antiviral agents | Investigational | | [29] |
| 392622 | Ritonavir | • HIV protease inhibitor<br>• Antiretroviral agent | Approved, Investigational | | [30] |
| 213039 | Darunavir | • HIV Protease Inhibitor | Approved | | [31] |
| 71661251 | Elbasvir | • Direct acting antiviral | Approved | | [32] |

| 49773361 | Beclabuvir | • Polymerase inhibitor of the hepatitis C virus (HCV) nonstructural protein 5B (NS5B) | Investigational | [33] |
| 151171 | Conivaptan | • Non-peptide inhibitor of antidiuretic hormone (vasopressin) | Approved, Investigational | [34] |
| 3663 | Hypericin | • Antineoplastic agents<br>• Antiviral agents<br>• Enzyme inhibitors<br>• Immunosuppressive agents<br>• Radiation-sensitizing agents<br>• Antidepressive agents | Investigational | [35] |
| 5362440 | Indinavir | • Antiretroviral drug for the treatment of HIV infection | Approved | [36] |
| 135398641 | Inosine | • Neuroprotective, cardioprotective, anti-inflammatory and immunomodulatory activities | Experimental, Investigational | [37] |
| 67505836 | Ledipasvir | • Direct-acting antiviral agent (DAAD) | Approved | [38] |

| 37723 | Lentinan | • Antineoplastic and immunomodulating agents | Experimental, Investigational | [39] |
| 64143 | Nelfinavir | • Anti-HIV agents<br>• HIV-1 protease inhibitor | Approved | [40] |
| 44424838 | Nystatin | • Antifungal agents<br>• Anti-mycotic agents | Approved, Vet approved | [41] |
| 441243 | Saquinavir | • HIV protease inhibitor | Approved, Investigational | [42] |
| 21704 | Vidarabine | • Nucleic acid inhibitor<br>• Antiviral agent<br>• Antimetabolites | Approved, Investigational | [43] |

## 2.4 Molecular docking and nonbond interaction analysis

Molecular docking is used to predict the predominant binding mode(s) of a drug with a protein of the known 3D structure [44]. In our study, molecular docking was carried out for the ligands against SARS-CoV-2 spike glycoprotein with AutoDock Vina wizard under PyRx software to screen the potential drug with a more negative binding affinity [10]. The lower the binding affinity, the better the drug-receptor complex is. The docked molecules' binding site and nonbond interaction were visualized in BIOVIA discovery studio visualizer (version: v20.1.0.19295) [45]. Molecular docking scores indicate the pharmaco-dynamic activity of the candidate drugs by scoring and orienting them to the receptor's binding site [46]. It is an indication of measuring the interaction of ligands to the active site of the targeted protein.

## 2.5 Study of pharmacokinetic parameters

The admetSAR@LMMD online database, MedChem Designer software was used to calculate the ADMET properties that include Absorption, Distribution, Metabolism, Excretion, and Toxicity of the compounds. Lipinski's rule described vital molecular properties for the pharmaco-kinetic activity of the ligands. These data also help to determine pharmacological activity and oral bioavailability of a drug [47, 48]. According to the rule, S + logP and S + logD value should be <5, and MlogP values must be <4.15. Here, logP reflects the partial coefficient of the molecule between an aqueous and lipophilic phase; logD reflects the total partition of both ionized and non-ionized forms of the compound; MlogP reflects the lipophilicity of a compound. The molecular weight should be <500 Da [49, 50].

# 3. Results and discussion

## 3.1 Binding energy analysis of protein-ligand complex by molecular docking

The docking is essential to predict the more robust binder and virtually screen a database of compounds. The ligands considered in this study showed negative binding energy. Thus, they are more likely to bind spontaneously without requiring any energy [13].

**Table 2.** Binding energy of collected drugs against spike glycoprotein of SARS-CoV-2 generated via flexible docking

| Compounds | Binding energy of ligand-protein (kcal/mol) | | | | |
| --- | --- | --- | --- | --- | --- |
| | 6LZG | 6VXX | 6X29 | 6YM0 | 6YOR |
| Beclabuvir | -7.7 | -7.6 | -8.7 | -7.2 | -7.2 |
| Conivaptan | -8.7 | -9.7 | -8.3 | -8.4 | -8.8 |
| Darunavir | -7.1 | -7.4 | -7.3 | -6.9 | -7.0 |
| Elbasvir | -8.1 | -8.6 | -8.3 | -7.8 | -8.4 |
| Hypericin | -9.4 | -9.0 | -9.1 | -8.9 | -8.8 |
| Indinavir | -7.5 | -7.5 | -8.3 | -6.8 | -7.3 |
| Inosine | -6.3 | -6.1 | -6.3 | -5.9 | -6.4 |
| Ledipasvir | -8.3 | -9.1 | -8.3 | -9.7 | -9.8 |
| Lentinan | -7.2 | -6.8 | -7.2 | -6.7 | -6.5 |
| Nelfinavir | -6.3 | -7.0 | -7.1 | -7.6 | -6.2 |
| Nystatin | -7.7 | -8.1 | -8.0 | -7.9 | -8.0 |
| Remdesivir | -6.6 | -7.2 | -7.4 | -6.8 | -7.5 |
| Ritonavir | -6.8 | -7.2 | -6.6 | -6.5 | -6.4 |
| Saquinavir | -7.6 | -7.9 | -6.6 | -7.6 | -8.2 |
| Vidarabine | -6.3 | -6.2 | -5.9 | -6.3 | -6.0 |
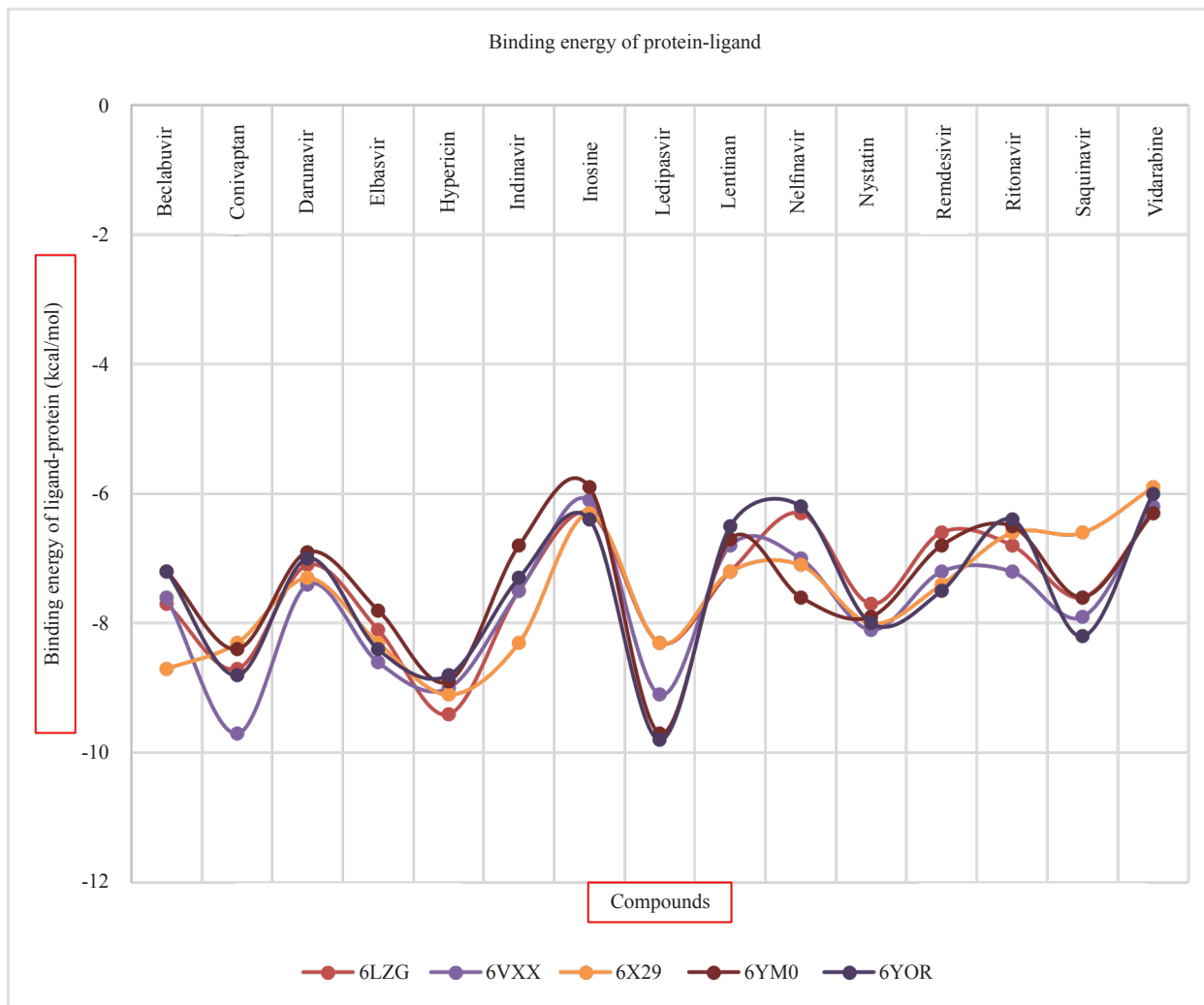
**Figure 1.** A graphical representation of the molecular docking results

In our study, Ledipasvir shows the strongest binding affinity (-9.8 kcal/mol) against protein code 6YOR by molecular docking. Conivaptan and Hypericin also predict better results with the protein code 6VXX and 6LZG, respectively. Among these 15 drugs, Beclabuvir, Conivaptan, Elbasvir, Hypericin, Ledipasvir, Nystatin, Saquinavir represent a promising results against target protein to inhibit COVID-19. Docking scores of all collected drugs against collected spike glycoprotein were tabulated in Table 2. A graphical chart for molecular docking results was shown in Figure 1.

### 3.2 *Nonbond interaction analysis of ligand-protein complex*

By analyzing docking results, it was explored that the interaction between Ledipasvir-6YOR, Ledipasvir-6YM0, Conivaptan-6VXX, Hypericin-6LZG, Hypericin-6X29, Ledipasvir-6VXX, and Hypericin-6VXX was most potent for inhibiting SARS-CoV-2. Nonbond interactions of these potential compounds against target protein were visualized in BIOVIA discovery studio visualizer (version: v20.1.0.19295) in Figure 2 and were tabulated in Table 3.

Hypericin shows the lowest binding energy against 6LZG protein, which is -9.4 Kcal/mol, followed by Conivaptan -8.7 Kcal/mol and Elbasvir -8.1 Kcal/mol shown in Table 2. Jacob Israelachvili & Richard Pashley described hydrophobic interactions decay exponentially with distance and best at 0-100 Å range [51]. Hypericin-6LZG complex shows hydrophobic bonds with PHE464 (4.82392), PHE464 (5.04822 Å), PHE464 (4.58984 Å), PHE464 (5.05938 Å),

PRO426 (4.77972 Å), PRO426 (5.32472 Å), PRO426 (5.28451 Å), PRO463 (4.21606 Å), and TYR396 (4.75356 Å) residues shown in Table 3.

| Compounds | Binding Energy (kcal/mol) | Hydrogen bonds (Amino acid Ligands) Distance (Å) | Hydrophobic Bonds (Amino acid Ligands) Distance (Å) | Halogen Bonds (Amino acid Ligands) Distance (Å) | Electrostatic Bonds (Amino acid Ligands) Distance (Å) |
|---|---|---|---|---|---|
| Ledipasvir-6YOR complex | -9.8 | ARG355 (2.89258) ARG355 (2.21921) GLU516 (3.73941) | ARG355 (4.43162) ARG466 (4.21209) VAL382 (4.27763) PHE392 (5.0249) TYR396 (5.38991) PHE464 (4.51494) | GLU516 (2.54603) | GLU516 (4.878) |
| Ledipasvir-6YM0 complex | -9.7 | ARG355 (2.97843) ARG355 (2.31537) LEU517 (2.62877) PHE464 (3.49521) | ARG355 (4.41457) ARG466 (4.32048) VAL382 (4.73363) TRP353 (4.79043) TYR396 (5.36667) PHE464 (4.48377) | GLU516 (2.82132) | GLU516 (4.87456) |
| Conivaptan-6VXX complex | -9.7 | ASN709 (1.84111) GLY1093 (2.30831) THR1077 (2.09954) | THR1077 (3.51505) VAL1094 (3.53247) PHE1089 (4.9845) PRO1079 (4.73657) ILE712 (5.08235) PRO1090 (5.43673) PRO1090 (5.45146) PRO1079 (4.18638) | | |
| Hypericin-6LZG complex | -9.4 | | PHE464 (4.82392) PHE464 (5.04822) PHE464 (4.58984) PHE464 (5.05938) PRO426 (4.77972) PRO426 (5.32472) PRO426 (5.28451) PRO463 (4.21606) TYR396 (4.75356) | | GLU516 (3.80465) |
| Hypericin-6X29 complex | -9.1 | PRO225 (2.96405) GLY283 (2.43948) PRO225 (2.61954) | TYR38 (4.54117) TYR38 (5.41022) TYR38 (4.2046) PRO225 (4.26092) | | GLU224 (4.76827) GLU224 (3.99043) |
| Ledipasvir-6VXX complex | -9.1 | SER708 (2.53207) | PRO1069 (4.0242) VAL1068 (5.35613) PRO1069 (5.45468) ALA713 (4.12458) ALA713 (3.91451) TYR1047 (4.83053) | | |
| Hypericin-6VXX complex | -9.0 | ASP428 (2.65801) ARG355 (2.58222) ARG355 (2.04507) SER514 (2.92458) | PHE464 (5.00675) PHE464 (4.6477) PHE464 (4.99753) PHE464 (5.15836) PHE464 (5.11649) PRO426 (4.79364) PRO463 (4.39894) PRO426 (5.11001) PRO426 (4.31555) PRO463 (4.60846) PHE464 (5.49099) | | |

Ledipasvir-6YOR interaction

Ledipasvir-6YM0 interaction

Conivaptan-6VXX interaction

Hypericin-6LZG interaction

Hypericin-6X29 interaction

Ledipasvir-6VXX interaction
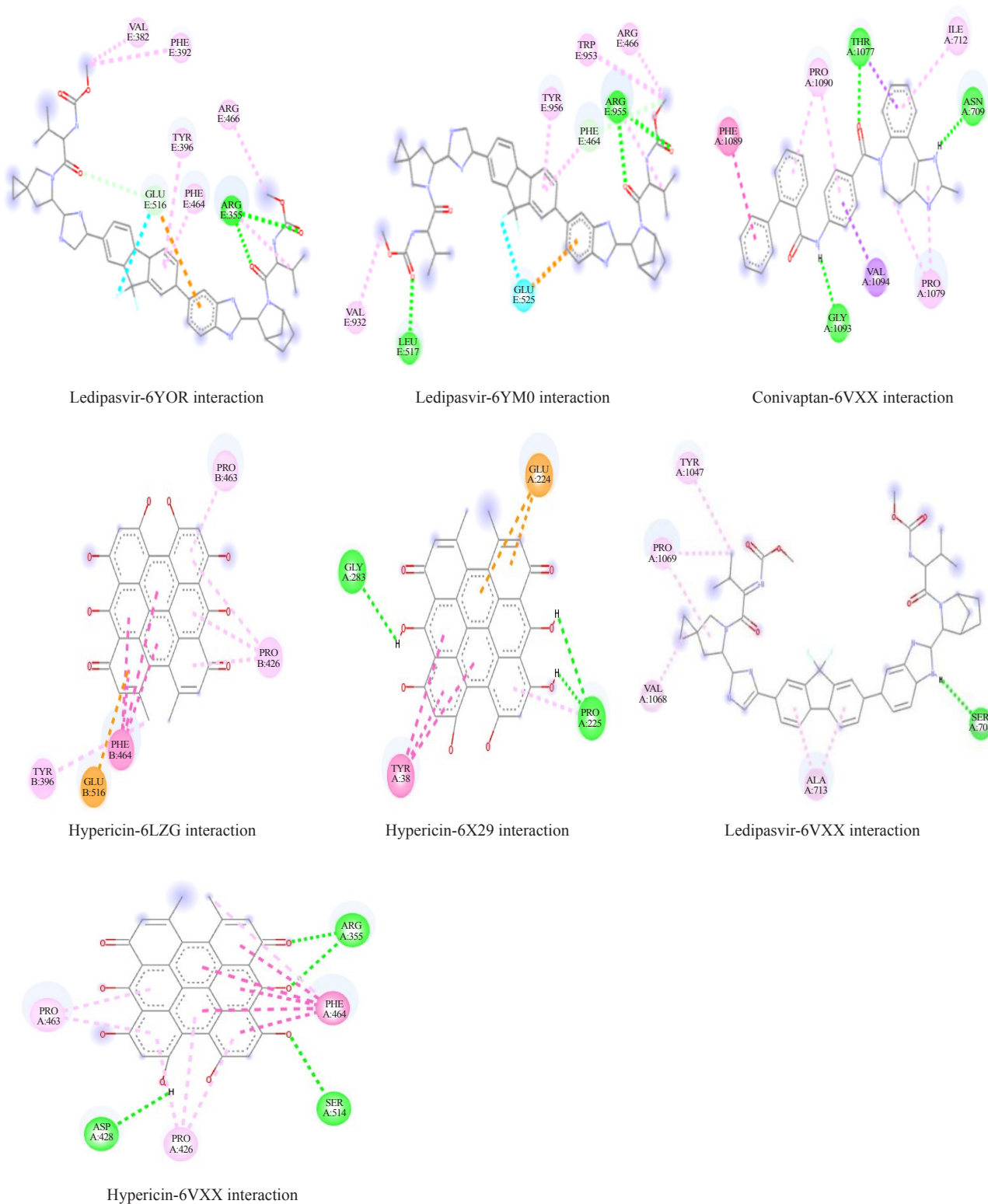
Hypericin-6VXX interaction

**Figure 2.** Nonbond interaction for potential drugs against target protein

Conivaptan exhibits the lowest binding energy against 6VXX, which is -9.7 Kcal/mol, followed by Ledipasvir -9.1 Kcal/mol and Hypericin -9.0 Kcal/mol. A hydrogen bond is essential for DNA structure and indicates that hydrogen

bond <2.3 Å increases the binding affinity by several magnitudes [52]. Strong H-bond is seen in ASN709 (1.84111 Å), GLY1093 (2.30831 Å), THR1077 (2.09954 Å) residues in Conivaptan-6VXX complex; SER708 (2.53207 Å) residues in Ledipasvir-6VXX complex; ASP428 (2.65801 Å), ARG355 (2.58222 Å), ARG355 (2.04507 Å), SER514 (2.92458 Å) residues in Hypericin-6VXX complex. Promising hydrophobic bonds have also been seen on Conivaptan-6VXX, Ledipasvir-6VXX, and Hypericin-6VXX complexes tabulated in Table 3.

A potential inhibitor against 6X29 glycoprotein is Hypericin with -9.1 Kcal/mol binding energy and H-bonds at PRO225 (2.96405 Å), GLY283 (2.43948 Å), PRO225 (2.61954 Å) residues. Hydrophobic bonds of Hypericin-6X29 complex are predicted in TYR38 (4.54117 Å), TYR38 (5.41022 Å), TYR38 (4.2046 Å), PRO225 (4.26092 Å) residues tabulated in Table 3.

Ledipasvir is a remarkable inhibitor of 6YM0 spike glycoprotein releasing -9.7 Kcal/mol energy while forming a complex. H-bonds are seen in ARG355 (2.97843 Å), ARG355 (2.31537 Å), LEU517 (2.62877 Å), PHE464 (3.49521 Å) residues of the complex. Strong hydrophobic bonds are seen at ARG355 (2.97843 Å), ARG355 (2.31537 Å), LEU517 (2.62877 Å), PHE464 (3.49521 Å) residues. Halogen and electro-static bond can be formed at GLU516 residue with 2.82132 Å and 4.87456 Å bond lengths (Table 3).

Ledipasvir binds 6YOR with exceptionally lower binding energy -9.8 Kcal/ mol, the lowest of all considered in the study. H-bonds are seen at ARG355 (2.89258 Å), ARG355 (2.21921 Å), GLU516 (3.73941 Å) residues. Strong hydrophobic bonds are seen at ARG355 (4.43162 Å), ARG466 (4.21209 Å), VAL382 (4.27763 Å), PHE392 (5.0249 Å), TYR396 (5.38991 Å), PHE464 (4.51494 Å) residues. Halogen and electro- static bond can be formed at GLU516 residue with GLU516 residue 2.54603 Å and 4.878 Å bond lengths.

### 3.3 *Pharmacokinetic activity analysis of the compounds*

The drug response to Blood Brain Barrier, Human Intestinal Absorption, Carco-2 Permeability, Pglycoprotein Inhibitor, Human Ether-a-go-go Related Gene Inhibitor and carcinogenic parameters is shown in Table 4. All the drugs except Lentinan and Nystatin show a satisfactory intestinal absorption. It is a major parameter of drug bioavailability [53]. P-glycoprotein can inhibit drug accumulation in the brain and facilitate drug excretion [54]. Hypericin, Inosine, Lentinan, Nystatin, Remdesivir, Vidarabine drugs are non-inhibitor of P-glycoprotein. Inhibition of Human Ether-a-go-go-Related Gene by drugs can induce ventricular arrhythmia and sudden cardiac death [55]. All the drugs in this study are weak inhibitors of the Human Ether-a-go-go-Related Gene. AdmetSAR@LMMD analysis shows that all the drugs are noncarcinogens. So the drugs are safe for administration.

Increased molecular weight can form a larger cavity in water to solubilize the compound. That's why the solubility of a compound decreases as the molecular weight increases [56]. Increased molecular weight indicates reduced intestinal absorption of the compound. All the drugs in the study have the molecular weight of more than 500 Da except Conivaptan, Inosine, and Vidarabine. So, the compounds Conivaptan, Inosine, Vidarabine can easily be absorbed in the intestine. Increased value of logP decreases aqueous solubility predicting reduced absorption of the compound [57]. All the compounds have MlogP value less than 4.5 and S + logP value less than 5, except Conivaptan, Elbasvir, Ledipasvir, and Hypericin. So, the compounds are hydrophilic in nature. The negative logP value indicates a more hydrophilic nature, indicating that the compounds Inosine, Lentinan, Nystatin, and Vidarabine show more hydrophilicity. They can be absorbed and excreted more quickly than other compounds. In the study, S + logD value of compounds also supports Lipinski's rule. According to the Lipinski's rule, The number of hydrogen bond donors should also be <5 [58]. The compounds maintain this rule except for Hypericin, Lentinan, Nystatin, and Saquinavir in our study. Pharmaco-kinetic proprieties of collected drugs obtained from MedChem Designer Software were given in Table 5.

### 3.4 *Hardness and softness analysis of potential drugs by calculating HOMO LUMO*

HOMO-LUMO GAP indicates the measurement of kinetic stability [59, 60]. HOMO-LUMO GAP is also closely related to the hardness and softness of the compounds. Larger Gap value suggests the hardness of the drug molecules, which is closely associated with the lower chemical reactivity and high kinetic stability. The smaller Gap value indicates the softness of the drug molecules, which signifies low kinetic stability and high chemical reactivity [60-62]. All the drugs in this study exhibit lower (<1.3) HOMO-LUMO GAP, indicating high chemical reactivity of the drugs described in Table 6. Indinavir shows the lowest GAP and most increased softness that might contribute to the significantly higher

reactivity of the drug molecule. Hypericin and Remdesivir also predict lower HOMO-LUMO GAP and higher softness. So, they are also chemically more reactive. HOMO-LUMO, gap, hardness and softness values were given in Table 6. The structure of frontier molecular orbitals (HOMO and LUMO) for the potential drugs were given in Figure 3.

**Table 4.** Selected pharmaco-kinetic parameters of drugs were obtained by using AdmetSAR@LMMD online database

| Compounds | Parameters | | | | | |
|---|---|---|---|---|---|---|
| | Blood-Brain Barrier | Human Intestinal Absorption | Caco-2 Permeability | Pglycoprotein Inhibitor | Human Ethera-go-go-Related Gene Inhibition | Carcinogens |
| Beclabuvir | BBB + 0.7783 | HIA + 1.0000 | Caco2 + 0.5434 | Inhibitor 0.6581 | Weak inhibitor 0.9111 | Non-carcinogens 0.6589 |
| Conivaptan | BBB + 0.9522 | HIA + 1.0000 | Caco2 + 0.5291 | Inhibitor 0.6901 | Weak inhibitor 0.9885 | Non-carcinogens 0.8831 |
| Darunavir | BBB - 0.5518 | HIA + 0.9636 | Caco2 + 0.7274 | Inhibitor 0.7588 | Weak inhibitor 0.9824 | Non-carcinogens 0.7991 |
| Elbasvir | BBB - 0.7263 | HIA + 0.9946 | Caco2 - 0.6459 | Inhibitor 0.7155 | Weak inhibitor 0.9077 | Non-carcinogens 0.9100 |
| Hypericin | BBB - 0.7368 | HIA + 0.9898 | Caco2 + 0.8019 | Non-inhibitor 0.8724 | Weak inhibitor 0.9198 | Non-carcinogens 0.8912 |
| Indinavir | BBB - 0.9923 | HIA+ 0.8210 | Caco2 - 0.8183 | Inhibitor 0.7987 | Weak inhibitor 0.9557 | Non-carcinogens 0.8870 |
| Inosine | BBB + 0.7979 | HIA + 0.9523 | Caco2 - 0.9070 | Non-inhibitor 0.9717 | Weak inhibitor 0.9855 | Non-carcinogens 0.9220 |
| Ledipasvir | BBB - 0.5848 | HIA + 0.9962 | Caco2 - 0.6818 | Inhibitor 0.7910 | Weak inhibitor 0.9938 | Non-carcinogens 0.9107 |
| Lentinan | BBB + 0.6207 | HIA - 0.8748 | Caco2 - 0.8836 | Non-inhibitor 0.7589 | Weak inhibitor 0.9517 | Non-carcinogens 0.9551 |
| Nelfinavir | BBB - 0.9659 | HIA+ 0.7472 | Caco2 - 0.7148 | Inhibitor 0.8121 | Weak inhibitor 0.9786 | Non-carcinogens 0.8547 |
| Nystatin | BBB - 0.9659 | HIA - 0.9308 | Caco2 - 0.7539 | Non-inhibitor 0.7322 | Weak inhibitor 0.9777 | Non-carcinogens 0.9682 |
| Remdesivir | BBB - 0.7452 | HIA + 0.8890 | Caco2 - 0.6599 | Non-inhibitor 0.7247 | Weak inhibitor 0.9295 | Non-carcinogens 0.8293 |
| Ritonavir | BBB - 0.9717 | HIA - 0.7195 | Caco2 - 0.8957 | Inhibitor 0.8317 | Weak inhibitor 0.9774 | Non-carcinogens 0.8664 |
| Saquinavir | BBB - 0.9949 | HIA + 0.7774 | Caco2 - 0.8957 | Inhibitor 0.8563 | Weak inhibitor 0.9687 | Non-carcinogens 0.8650 |
| Vidarabine | BBB + 0.9383 | HIA + 0.9227 | Caco2 - 0.8957 | Non-inhibitor 0.9660 | Weak inhibitor 0.9890 | Non-carcinogens 0.9182 |

**Table 5.** Pharmaco-kinetic proprieties of collected drugs were obtained from MedChem Designer Software

| Compounds | Pharmaco-kinetic parameters | | | | |
|---|---|---|---|---|---|
| | M Wt | MlogP | S + logP | S + logD | HBDH |
| Beclabuvir | 659.853 | 3.757 | 3.846 | 3.583 | 1.000 |
| Conivaptan | 498.588 | 4.375 | 6.240 | 6.237 | 2.000 |
| Darunavir | 547.674 | 1.607 | 1.932 | 1.932 | 4.000 |
| Elbasvir | 882.038 | 3.031 | 6.315 | 6.313 | 4.000 |
| Hypericin | 504.456 | 1.979 | 5.019 | 1.741 | 6.000 |
| Indinavir | 613.805 | 1.725 | 2.779 | 2.706 | 4.000 |
| Inosine | 268.230 | -2.138 | -1.956 | -1.960 | 4.000 |
| Ledipasvir | 889.021 | 4.105 | 6.642 | 6.641 | 4.000 |
| Lentinan | 1153.018 | -12.461 | -7.551 | -7.551 | 23.000 |
| Nelfinavir | 567.796 | 3.242 | 4.598 | 4.571 | 4.000 |
| Nystatin | 926.116 | -1.752 | -1.769 | -1.796 | 13.000 |
| Remdesivir | 602.588 | 0.634 | 1.597 | 1.597 | 5.000 |
| Ritonavir | 720.958 | 2.267 | 4.205 | 4.204 | 4.000 |
| Saquinavir | 670.857 | 2.143 | 3.538 | 3.497 | 6.000 |
| Vidarabine | 267.246 | -1.545 | -1.059 | -1.059 | 5.000 |

**Table 6.** Energy of HOMOs, LUMOs, gap, hardness, and softness of following compounds were obtained from WebMO online database

| Molecules | $\varepsilon$HOMO | $\varepsilon$LUMO | GAP | Hardness ($\eta$) | Softness (S) |
|---|---|---|---|---|---|
| Beclabuvir | -0.127 | 0.191 | 0.318 | 0.159 | 6.289 |
| Conivaptan | -0.823 | 0.317 | 1.14 | 0.57 | 1.754 |
| Darunavir | -0.150 | 0.104 | 0.254 | 0.127 | 7.874 |
| Hypericin | -0.109 | 0.099 | 0.208 | 0.104 | 9.615 |
| Indinavir | -0.047 | 0.071 | 0.118 | 0.059 | 16.949 |
| Inosine | -0.368 | 0.741 | 1.109 | 0.5545 | 1.803 |
| Nelfinavir | -0.143 | 0.122 | 0.265 | 0.1325 | 7.547 |
| Remdesivir | -0.197 | 0.012 | 0.209 | 0.1045 | 9.569 |
| Vidarabine | -1.047 | 0.188 | 1.235 | 0.6175 | 1.619 |
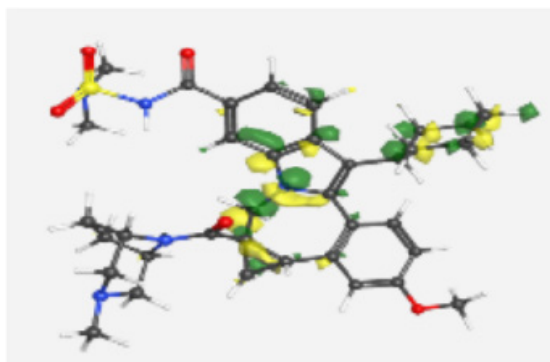
Beclabuvir-HOMO
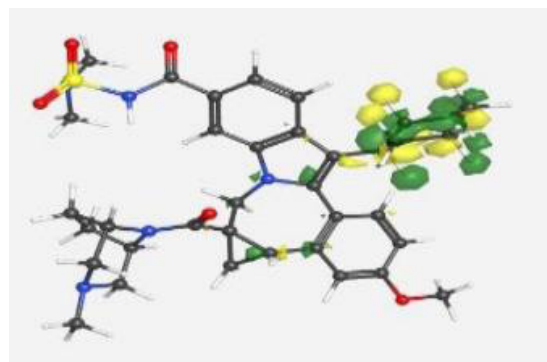
Beclabuvir-LUMO
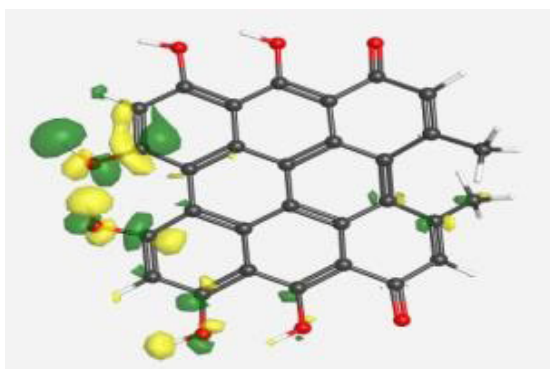
Hypericin-HOMO
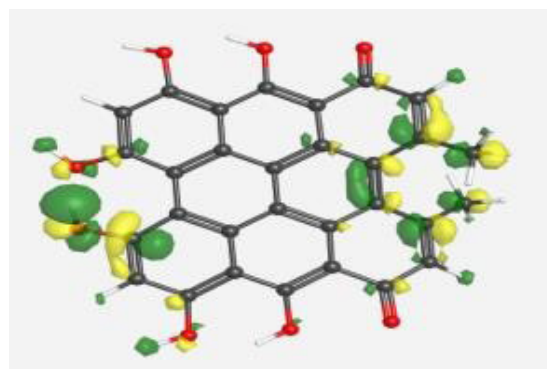
Hypericin-LUMO
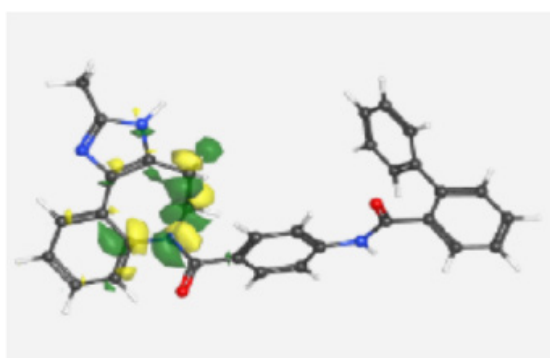
Conivaptan-HOMO
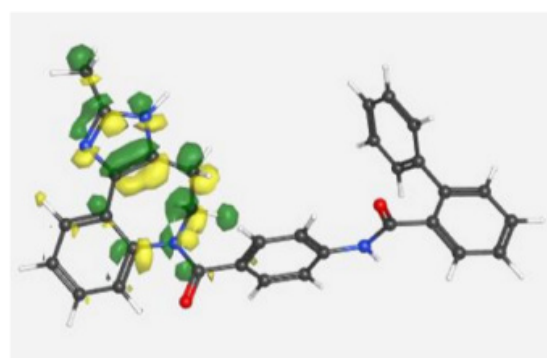
Conivaptan-LUMO
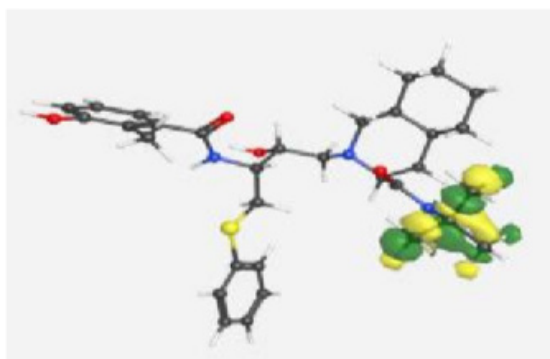
Nelfinavir-HOMO
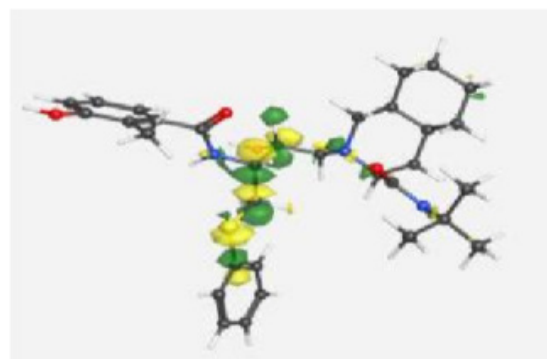
Nelfinavir-LUMO

**Figure 3.** Frontier molecular orbitals (HOMO and LUMO) of the potential drugs

# 4. Conclusion

This study demonstrated Beclabuvir, Conivaptan, Darunavir, Elbasvir, Hypericin, Indinavir, Inosine, Ledipasvir, Lentinan, Nelfinavir, Nystatin, Remdesivir, Ritonavir, Saquinavir, Vidarabine bind with 6LZG, 6VXX, 6X29, 6YM0, 6YOR proteins of SARS-CoV-2 and some important properties of drugs related to HOMO-LUMO energy GAP, hardness-softness by molecular orbital calculation. The drug showed the lowest binding energy and H-bonds, hydrophilic bonds, halogen bonds, and electrostatic bonds with almost all the targeted proteins of SARS-CoV-2 with a minimum of exception. The docking results of Ledipasvir, followed by Hypericin, show that they might perform better on inhibiting the targeted proteins. The nonbonding interactions analysis made it evident that 6VXX is a promising drug target as Conivaptan, Ledipasvir, and Hypericin can effectively target the protein. All drugs are non-carcinogenic shown from the pharmacokinetic calculation. We can state that, among the other ligands considered in this study, Ledipasvir might be the best ligand against SARS-CoV-2 induced infections for future researchers.

# Acknowledgment

# Author contributions

This work is a collaboration among all the authors. All authors contributed equally.

# Conflicts of interest

The authors declare no competing financial interest.

# Reference

[1] Huang C, Wang Y, Li X, Ren L, Zhao J, Hu Y, et al. Clinical features of patients infected with 2019 novel coronavirus in Wuhan, China. *Lancet*. 2020; 395(10223): 497-506.
[2] WHO. World Health Organization. Naming the coronavirus disease (COVID-19) and the virus that causes it. 2020. Available from: https://www.who.int/emergencies/diseases/novel-coronavirus-2019/technical-guidance/naming-the-coronavirus-disease-(covid-2019)-and-the-virus-that-causes-it [Accessed 6th November 2021].
[3] Johns Hopkins Hospital and Medicine. *Coronavirus COVID-19 Global Cases by the Center for Systems Science and Engineering (CSSE) at Johns Hopkins University (JHU)*. Johns Hopkins University. 2020.
[4] WHO. *Q & As on COVID-19 and related health topics*. World Health Organization. 2020.
[5] Emmanuel C. Coronaviruses with SARS-CoV-2 (causative agent for COVID-19) as a case study. 2020. Available from: doi: 10.13140/RG.2.2.31080.42242.
[6] Bosch BJ, van der Zee R, de Haan CAM, Rottier PJM. The coronavirus spike protein is a class I virus fusion protein: Structural and functional characterization of the fusion core complex. *Journal of Virology*. 2003; 77(16): 8801-8811.
[7] Wu C, Liu Y, Yang Y, Zhang P, Zhong W, Wang Y, et al. Analysis of therapeutic targets for SARS-CoV-2 and discovery of potential drugs by computational methods. *Acta Pharmaceutica Sinica B*. 2020; 10(5): 766-788.
[8] Ou X, Liu Y, Lei X, Li P, Mi D, Ren L, et al. Characterization of spike glycoprotein of SARS-CoV-2 on virus entry and its immune cross-reactivity with SARS-CoV. *Nature Communications*. 2020; 11(1): 1620.
[9] Krusemark CJ. Drug design: Structure- and ligand-based approaches. *The Quarterly Review of Biology*. 2012; 87(2): 176.

[10] Trott O, Olson AJ. AutoDock Vina: Improving the speed and accuracy of docking with a new scoring function, efficient optimization, and multithreading. *Journal of Computational Chemistry*. 2010; 31(2): 455-461.

[11] Dar AM, Mir S. Molecular docking: Approaches, types, applications and basic challenges. *Journal of Analytical & Bioanalytical Techniques*. 2017; 8: 1000356. Available from: doi: 10.4172/2155-9872.1000356.

[12] Schneider G, Böhm HJ. Virtual screening and fast automated docking methods. *Drug Discovery Today*. 2002; 7(1): 64-70.

[13] Lehn JM. Supramolecular chemistry: From molecular recognition towards molecular information processing and self-organization. *Materials Science Forum*. 1992. Available from: https://doi.org/10.4028/www.scientific.net/MSF.91-93.100 [Accessed 6th November 2021].

[14] Alberts B, Johnson A, Lewis J, et al. Analyzing protein structure and function. In: *Molecular Biology of the Cell*. New York: Garland Science; 2002.

[15] Madej T, Lanczycki CJ, Zhang D, Thiessen PA, Geer RC, Marchler-Bauer A, et al. MMDB and VAST+: Tracking structural similarities between macromolecular complexes. *Nucleic Acids Research*. 2014; 42(Database issue): D297-303.

[16] Gui M, Song W, Zhou H, Xu J, Chen S, Xiang Y, et al. Cryo-electron microscopy structures of the SARS-CoV spike glycoprotein reveal a prerequisite conformational state for receptor binding. *Cell Research*. 2017; 27(1): 119-129.

[17] Kim S, Chen J, Cheng T, Gindulyte A, He J, He S, et al. PubChem 2019 update: Improved access to chemical data. *Nucleic Acids Research*. 2019; 47(D1): D1102-D1109.

[18] Wang Q, Zhang Y, Wu L, Niu S, Song C, Zhang Z, et al. Structural and functional basis of SARS-CoV-2 entry by using human ACE2. *Cell*. 2020; 181(4): 894-904.

[19] Walls AC, Park YJ, Tortorici MA, Wall A, McGuire AT, Veesler D. Structure, function, and antigenicity of the SARS-CoV-2 spike glycoprotein. *Cell*. 2020; 181(2): 281-292.

[20] Henderson R, Edwards RJ, Mansouri K, Janowska K, Stalls V, Gobeil S, et al. Controlling the SARS-CoV-2 spike glycoprotein conformation. *Nnature Structural & Molecular Biology*. 2020; 27: 925-933. Available from: doi: 10.1038/s41594-020-0479-4.

[21] *6YM0: Crystal structure of the SARS-CoV-2 receptor binding domain in complex with CR3022 Fab (crystal form 1)*. Available from: https://www.ncbi.nlm.nih.gov/Structure/pdb/6YM0 [Accessed 6th November 2021].

[22] *6YOR: Structure of the SARS-CoV-2 spike S1 protein in complex with CR3022 Fab*. Available from: https://www.ncbi.nlm.nih.gov/Structure/pdb/6YOR [Accessed 6th November 2021].

[23] Lill MA, Danielson ML. Computer-aided drug design platform using PyMOL. *Journal of Computer-Aided Molecular Design*. 2011; 25(1): 13-19.

[24] Guex N, Peitsch MC, Schwede T. Automated comparative protein structure modeling with SWISS-MODEL and Swiss-PdbViewer: A historical perspective. *Electrophoresis*. 2009; 30(1): 162-173.

[25] Pearson RG. Absolute electronegativity and hardness correlated with molecular orbital theory. *Proceedings of the National Academy of Sciences of the United States of America*. 1986; 83(22): 8440-8441.

[26] Aihara JI. Reduced HOMO-LUMO gap as an index of kinetic stability for polycyclic aromatic hydrocarbons. *The Journal of Physical Chemistry A*. 1999; 103(37): 7487-7495.

[27] Pearson RG. The HSAB Principle-more quantitative aspects. *Inorganica Chimica Acta*. 1995; 240(1-2): 93-98.

[28] Ayers PW, Parr RG, Pearson RG. Elucidating the hard/soft acid/base principle: A perspective based on half-reactions. *The Journal of Chemical Physics*. 2006; 124(19): 194107. Available from: doi: 10.1063/1.2196882.

[29] PubChem. Remdesivir | C27H35N6O8P. Available from: https://pubchem.ncbi.nlm.nih.gov/compound/121304016 [Accessed 1st July 2020].

[30] PubChem. Ritonavir | C37H48N6O5S2. Available from: https://pubchem.ncbi.nlm.nih.gov/compound/392622 [Accessed 1st July 2020].

[31] PubChem. Darunavir | C27H37N3O7S. Available from: https://pubchem.ncbi.nlm.nih.gov/compound/213039#section=2D-Structure [Accessed 1st July 2020].

[32] PubChem. Elbasvir | C49H55N9O7. Available from: https://pubchem.ncbi.nlm.nih.gov/compound/71661251#section=Structures [Accessed 1st July 2020].

[33] PubChem. Beclabuvir | C36H45N5O5S. Available from: https://pubchem.ncbi.nlm.nih.gov/compound/49773361 [Accessed 1st July 2020].

[34] PubChem. Conivaptan | C32H26N4O2. Available from: https://pubchem.ncbi.nlm.nih.gov/compound/151171 [Accessed 1st July 2020].

[35] PubChem. Hypericin | C30H16O8. Available from: https://pubchem.ncbi.nlm.nih.gov/compound/3663 [Accessed

1st July 2020].

[36] PubChem. Indinavir | C36H47N5O4. Available from: https://pubchem.ncbi.nlm.nih.gov/compound/5362440 [Accessed 1st July 2020].

[37] PubChem. Inosine | C10H12N4O5. Available from: https://pubchem.ncbi.nlm.nih.gov/compound/135398641 [Accessed 1st July 2020].

[38] PubChem. Ledipasvir | C49H54F2N8O6. Available from: https://pubchem.ncbi.nlm.nih.gov/compound/67505836 [Accessed 1st July 2020].

[39] PubChem. Lentinan | C42H72O36. Available from: https://pubchem.ncbi.nlm.nih.gov/compound/37723 [Accessed 1st July 2020].

[40] PubChem. Nelfinavir | C32H45N3O4S. Available from: https://pubchem.ncbi.nlm.nih.gov/compound/64143 [Accessed 1st July 2020].

[41] PubChem. Nystatin | C47H75NO17. Available from: https://pubchem.ncbi.nlm.nih.gov/compound/44424838 [Accessed 1st July 2020].

[42] PubChem. Saquinavir | C38H50N6O5. Available from: https://pubchem.ncbi.nlm.nih.gov/compound/441243 [Accessed 1st July 2020].

[43] PubChem. Vidarabine | C10H13N5O4. Available from: https://pubchem.ncbi.nlm.nih.gov/compound/21704 [Accessed 1st July 2020].

[44] Morris GM, Lim-Wilby M. Molecular docking. *Methods in Molecular Biology*. 2008; 443: 365-382.

[45] Miyata T. Discovery studio modeling environment. *Ensemble*. 2015. Available from: https://scholar.google.com/scholar?hl=en&as_sdt=0%2C5&q=Miyata+T.+Discovery+studio+modeling+environment.+Ensemble.+2015%3B+&btnG= [Accessed 9th November 2021].

[46] Nithya G, Ilakkia A, Sakthisekaran D. In silico docking studies on the anti-cancer effect of thymoquinone on interaction with phosphatase and tensin homolog located on chromosome 10q23: A regulator of PI3K/AKT pathway. *Asian Journal of Pharmaceutical and Clinical Research*. 2015; 8(1): 192-195.

[47] Thais BF, Mariana CFS, Michelle CP, Roberto PF. Analysis of the applicability and use of lipinski's rule for central nervous system drugs. *Letters in Drug Design & Discovery*. 2016; 13(10): 999-1006.

[48] Barreiro EJ, Kümmerle AE, Fraga CAM. The methylation effect in medicinal chemistry. *Chemical Reviews*. 2011; 111(9): 5215-5246.

[49] Walters WP. Going further than Lipinski's rule in drug design. *Expert Opinion on Drug Discovery*. 2012; 7(2): 99-107.

[50] Doak BC, Kihlberg J. Drug discovery beyond the rule of 5-Opportunities and challenges. *Expert Opinion on Drug Discovery*. 2017. 12(2): 115-119.

[51] Israelachvili J, Pashley R. The hydrophobic interaction is long range, decaying exponentially with distance. *Nature*. 1982; 300(5890): 341-342.

[52] Wade RC, Goodford PJ. The role of hydrogen-bonds in drug binding. *Progress in Clinical and Biological Research*. 1989; 289: 433-444.

[53] Pang KS. Modeling of intestinal drug absorption: Roles of transporters and metabolic enzymes (for the gillette review series). *Drug Metabolism and Disposition*. 2003; 31(12): 1507-1519.

[54] Tanigawara Y. Role of P-glycoprotein in drug disposition. *Therapeutic Drug Monitoring*. 2000; 22(1): 137-140.

[55] Huang XP, Mangano T, Hufeisen S, Setola V, Roth BL. Identification of human Ether-à-go-go related gene modulators by three screening platforms in an academic drug-discovery setting. *ASSAY and Drug Development Technologies*. 2010; 8(6): 727-742.

[56] Hopkins AL, Paolini GV. Chemogenomics in drug discovery-the druggable genome and target class properties. In: *Comprehensive Medicinal Chemistry II*. 2006. Available from: doi: 10.1016/B0-08-045044-X/00260-1.

[57] Arabi AA. Routes to drug design via bioisosterism of carboxyl and sulfonamide groups. *Future Medicinal Chemistry*. 2017; 9(18): 2167-2180. Available from: http://www.future-science.com/doi/10.4155/fmc-2017-0136 [Accessed 9th November 2021].

[58] Lipinski CA, Lombardo F, Dominy BW, Feeney PJ. Experimental and computational approaches to estimate solubility and permeability in drug discovery and development settings. *Advanced Drug Delivery Reviews*. 2012; 46(1-3): 3-26.

[59] Aihara JI. Correlation found between the HOMO-LUMO energy separation and the chemical reactivity at the most reactive site for isolated-pentagon isomers of fullerenes. *Physical Chemistry Chemical Physics*. 2000; 14 (2): 3121-3125.

[60] Ullah MA, Johora FT, Sarkar B, Araf Y, Ahmed N, Nahar AN, et al. Computer-assisted evaluation of plant-derived

β-secretase inhibitors in Alzheimer's disease. *Egyptian Journal of Medical Human Genetics*. 2021; 22: 26.

[61] Sarkar B, Alam S, Rajib TK, Islam SS, Araf Y, Ullah MA. Identification of the most potent acetylcholinesterase inhibitors from plants for possible treatment of Alzheimer's disease: a computational approach. *Egyptian Journal of Medical Human Genetics*. 2021; 22: 10.

[62] Ullah MA, Johora FT, Sarkar B, Araf Y, Rahman MH. Curcumin analogs as the inhibitors of TLR4 pathway in inflammation and their drug like potentialities: A computer-based study. *Journal of Receptors and Signal Transduction*. 2020; 40(4): 324-338.